Master thesis

Excited States in ^{103}Sn

by

Lars-Erik Berglund

Supervisor: Prof. Claes Fahlander

Department of Physics
Division of Cosmic and Subatomic Physics
Lund University
Sölvegatan 14, 223 62 Lund
February 2000

ABSTRACT

The ^{103}Sn nucleus has been studied using data from a EUROBALL experiment. The experimental technique used was based on the detection of γ-rays in coincidence with light evaporated particles. The fusion-evaporation reaction ^{58}Ni + ^{54}Fe formed the compound nucleus ^{112}Xe which then decayed by the emission of α-particles, protons and neutrons. γ-ray lines from ^{103}Sn have been identified for the first time and a level scheme of ^{103}Sn has been established.

CONTENTS

1 INTRODUCTION

The neutron deficient nucleus $^{103}_{50}Sn_{53}$ is interesting for several reasons. The main reason is that ^{103}Sn is in the vicinity of $^{100}_{50}Sn_{50}$, the heaviest so called doubly magic nucleus with equal number of protons and neutrons. A nucleus with a magic number of protons or/and neutrons is more tightly bound than other nuclei and it has been established already in the early 1950's that the nucleons in such magic nuclei exhibit shell properties. The theoretical nuclear shell model is in good agreement with experimental results from nuclei with filled or almost filled shells and by studying nuclei close to ^{100}Sn, it is possible to deduce interesting properties necessary for the nuclear shell model. Research has previously been made in the ^{100}Sn region and it has given rise to two doctor theses in the Lund group [1,2]. The interested readers id referred to these works.

^{103}Sn is very neutron deficient, i.e. it lies far away from β^- stability line. It is therefore extremly difficult to identify energy transitions in ^{103}Sn, since the cross section for producing it is small. To succed in identifying excited states in ^{103}Sn and to discriminate the weakly populated ^{103}Sn channel from strongly populated channels it has therefore been necessary to detect and measure not only γ-rays but also particles such as protons, neutrons and α-particles which are emitted in the decay process.

The aim of the analysis was to establish a level scheme of ^{103}Sn which has been done. Six energy transitions in ^{103}Sn have been identified, which give us information about energy, parity and angular momentum of the excited states.

2 THE EXPERIMENT

2.1 Nuclear Reactions

The aim of the experiment was to investigate the ^{103}Sn isotope and its possible excited states. ^{103}Sn was populated in a reaction using ^{58}Ni as the projectile and ^{54}Fe as the target. The result of this heavy-ion fusion evaporation reaction is the compound nucleus, ^{112}Xe. Both energy and angular momentum is transfered to the compound nucleus. It is formed in a highly excited state (see figure 1), which will decay promptly by first emitting a number of particles. In the figure the yrast line is indicated. The definition of an yrast state is the state that, for a given value of angular momentum, has the lowest energy [3].

The particle emission occurs in a variety of different ways, but the decay probability of the compound nucleus depends only on the total energy and angular momentum given to the system and not in the way it was formed in the fusion reaction [3]. The decay process is governed by statistical rules.

Thus, after the formation of the excited compound nucleus it first cools down by evaporation of light particles such as protons, α-particles and neutrons according to:

$$^{58}_{28}\mathrm{Ni} + {}^{54}_{26}\mathrm{Fe} \rightarrow {}^{112}_{54}\mathrm{Xe}^{*} \rightarrow \mathrm{xp} + \mathrm{yn} + \mathrm{z}\alpha + {}^{A}_{Z}\mathrm{X}$$

About 30 different reaction channels may be open. The reactions induced by heavy ions produce compound nuclei of very high angular momentum [3]. The evaporated particles carry away both energy and angular momenta. However, there is still a considerable amount of those quantities left in the residual nucleus after particle evaporation, since at

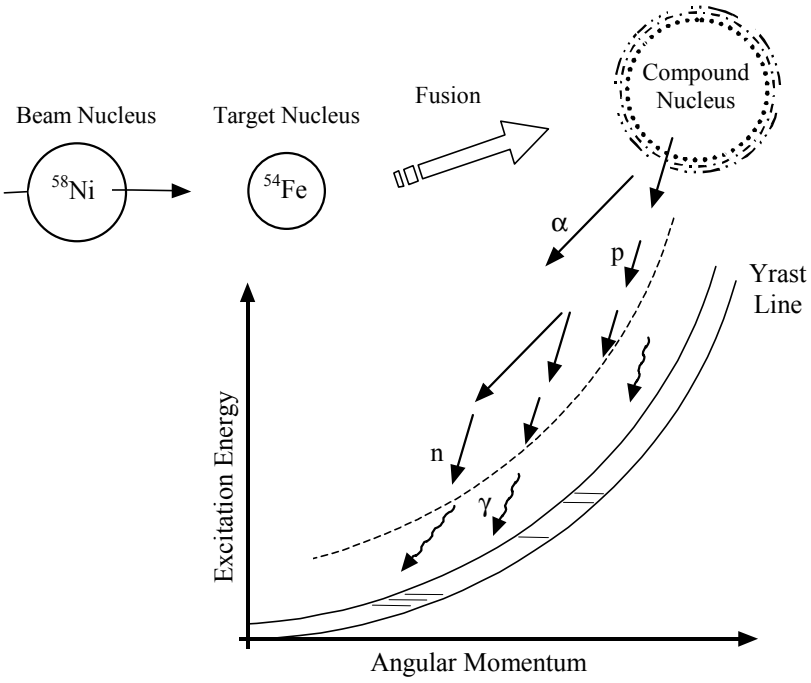

Figure 1: Excitation energy and angular momentum of levels in the compound nucleus produced in a heavy-ion reaction.

some point, at about 8 MeV of excitation energy, the energy left in the system is not enough to overcome the binding energy of the particle. A dashed line in figure 1 indicates the limit for particle emission.

When the particle emission is no longer energetically possible, the final product nucleus (residual nucleus) instead gets rid of the excess energy and angular momentum by emitting a cascade of nuclear electromagnetic radiation; γ-rays. At high excitation energies the density of states is high, and the lifetime of the states is short due to the large number of decay paths. This first part of the γ-ray emission therefore gives rise to a continuum spectrum. It is not until the decay reaches close to the yrast line that a cascade of discrete γ-ray transitions can be seen de-excitating the residual nucleus from levels close to the yrast levels. The total process, from the collision till the populated nucleus is in the ground state, is completed very quickly, in about 10^{-9} seconds, unless there is an isomeric state along the decay path.

Figure 2 shows a part of the nuclidic chart of the different reaction channels which were open in the present experiment. Top right is the compound nucleus ^{112}Xe. Every channel corresponds to a nucleus. For instance; ^{105}In is produced by the emission of one α-particle and three protons (the 1α3p channel), ^{102}Cd is produced through the 2α2p channel and ^{103}Sn e.g. is produced through the 2α1n channel.

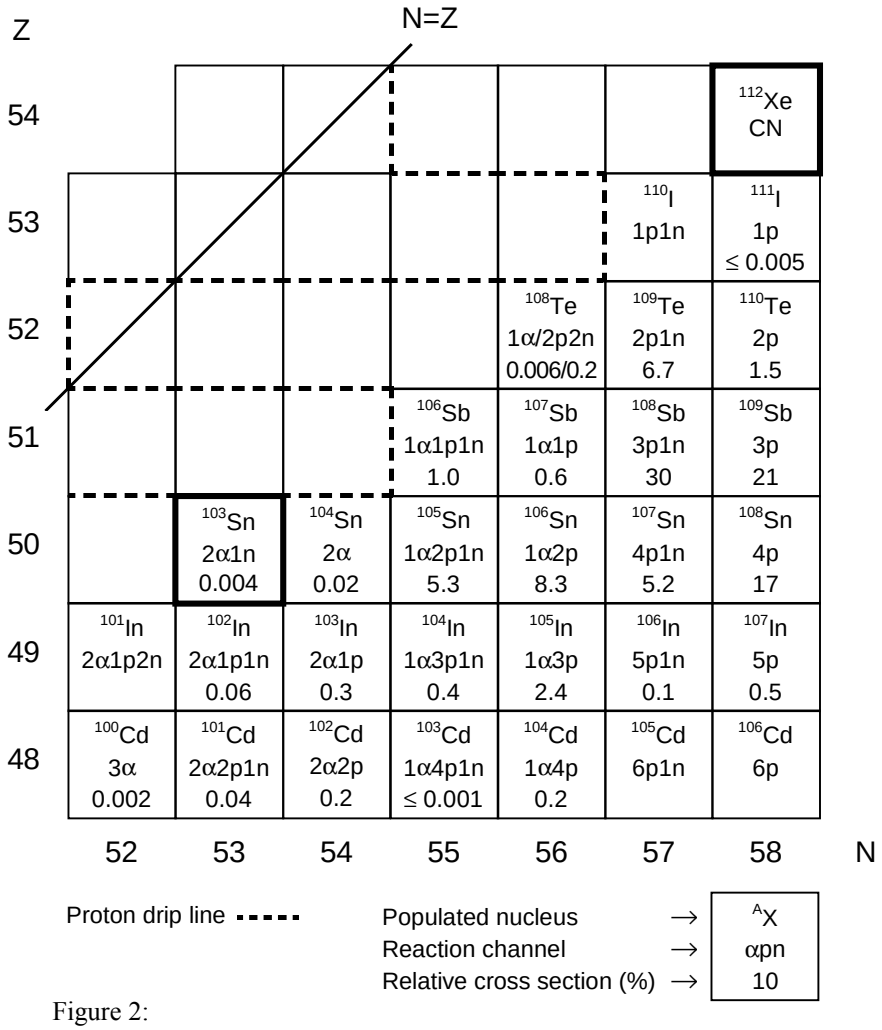

Figure 2:
Part of the nuclidic chart showing the nuclei indentified in the experiment.

Some of the nuclei can be produced through two different reaction channels. For example ^{108}Te, which was produced by the emission of one α-particle or by two protons and two neutrons (see figure 2).

The relative experimental cross section (in %), i.e. the probability for a nucleus to be populated, is also indicated in the figure. They were determined in the project work, which will be discussed in section 3.3. The dashed line in the figure is the expected proton drip line, i.e. the border between nuclei where the ground state decay is governed by slower processes and those that can emit protons from their ground states.

Some channels are strong and some are very weak as can be seen in figure 2. The 3p1n reaction channel leading to ^{108}Sb is the strongest channel, populated in about 30 % of all reactions, whereas ^{103}Sn e.g. is populated in only about 0.004 % of all the reactions. Since the compound nucleus ^{112}Xe is relatively proton rich the emitted particles are dominated by protons, which bring the residual nucleus towards the stability line. Because of this proton excess the separation energy for the neutrons is much higher than for the protons and therefore the emission of neutrons is very rare in the reactions. The residual nuclei close to the proton drip line are mainly produced with α-particle and neutron evaporation, which are weak channels. The most interesting events are representated by very weak reaction channels.

2.2 Experimental Setup

The data set that was used for the analysis in this work was obtained from an experiment carried out in autumn 1998 at the accelerator laboratory of Laboratori Nazionali di Legnaro in Italy.

In the Tandem Van de Graaff XTU accelerator negative ^{58}Ni ions were produced and then accelerated in an electric field toward a high-voltage terminal (see figure 3). Passing through a thin foil of ^{12}C the ions were stripped of electrons and the beam could after the passage continue the acceleration of the now positive ions in the potential difference. However, there will be a distribution of the charge of the ions given that the ions leave the terminal with different enegies. In an analyzing magnet, where ions with too much or too little energy declines (see figure 3), the final energy, 240 MeV, was selected.

The avergage beam intensity was measured to about 2 particle nA and the number of incident particles per second, n, was thus about 10^{10} s^{-1}.

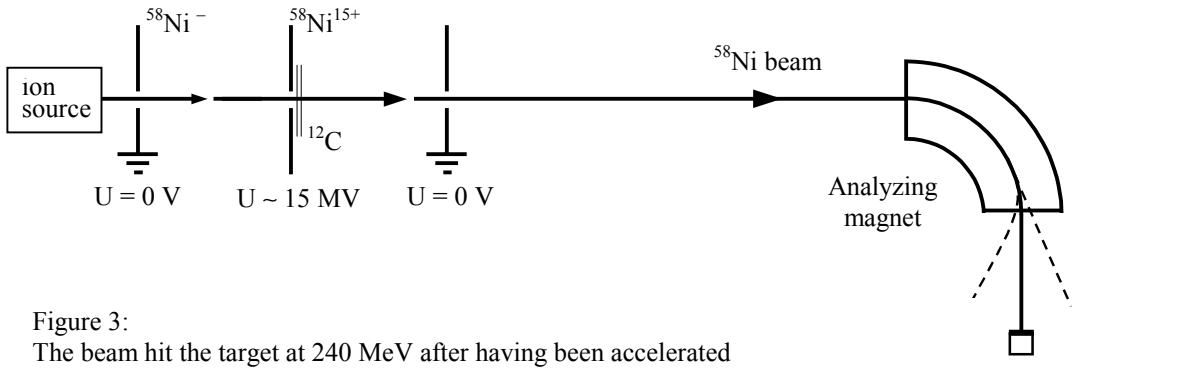

Figure 3:
The beam hit the target at 240 MeV after having been accelerated twice over a potential fall of 15 MV.

The target, an ^{54}Fe foil with a thickness of 1.4 mg/cm^2, was enriched to 99.915 % and evaporated onto a Au backing of thickness 13.3 mg/cm^2. There were impurities from ^{56}Fe (0.06 %), ^{57}Fe (0.02 %) and ^{58}Fe (< 0.05 %) in the target. Such a very high enrichment is important when nuclei far from stability are to be investigated. The cross sections for such reactions are very small and details of target purity become of utmost importance.

Since it is not possible to get perfect vacuum build up of oxygen on the target is sometimes a problem. Also because of oil from the vacuum pumps there may also be problems with carbon build ups. Such impurities in the target will cause unwanted reactions contributing to the background in the γ-ray spectra. In this experiment there was not much of carbon build up but a considerable build-up of ^{16}O took place on the target during the experiment. The presence of ^{65}Ge e.g. in some of the spectra have their origin from the 2α1n channel of the reaction ^{58}Ni + ^{16}O.

There will be a recoil of the compound nucleus in heavy ion fusion-evaporation reactions. This recoil causes a motion of the emitting nuclei. We get a Doppler effect which broadens the measured γ-ray lines. The thick Au backing was used in order to stop the evaporation residues and minimize the Doppler effect of the residual nuclei.

The ratio of the number of colliding particles per second, the reaction rate R, and the number of incident particles per second n, is equal to the ratio of the sum of the collision cross sections, and the whole area [4]:

$$\frac{R}{n} = \frac{NSx\sigma}{S} \Rightarrow R = nNx\sigma = \frac{nN_A x\sigma}{A} \approx 10^5 s^{-1}$$

where N is the number of target nuclei per cubic centimetre of target, S is the surface of the target, x is the target thickness, N_A is Avogadro's number, A is the mass number and σ is the total reaction cross section. σ was estimated to about 0.5 b (see section 3.3).

The experiment required five days of beam-time.

2.3 Detectors

The experiment was performed using the EUROBALL detector system, which is a newly developed multi-detector system for detection of γ-rays. In studies of excited states in ^{103}Sn γ-rays are the most important quantities to measure. However, due to the many strong reaction channels (see figure 2), and the extremly small cross section for ^{103}Sn, it is absolutely necessary to detect the light particles emitted in the reaction to succed in identifying ^{103}Sn. In the present experiment a technique based on the detection of γ-rays in coincidence with light evaporated particles was used. The EUROBALL detector array was therefore complemented with two sorts of ancillery detectors, namely a Si ball for detection of charged particles, i.e. protons and α-particles, and a neutron-wall for detecting neutrons (see figure 4).

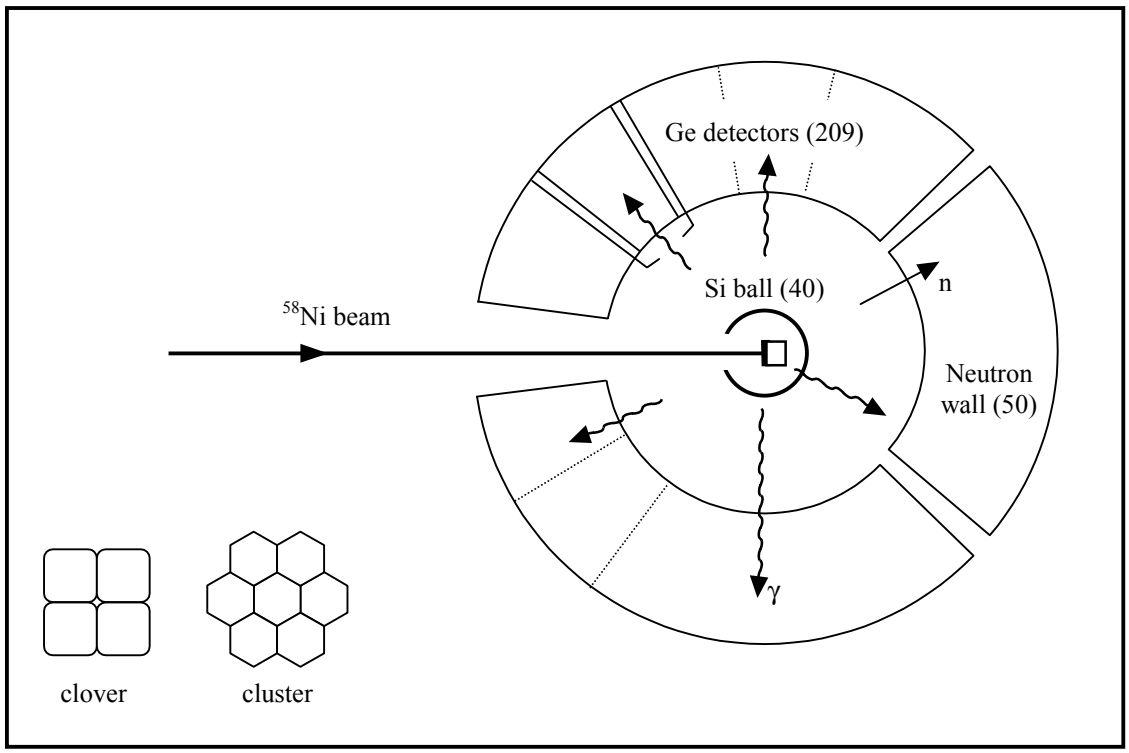

Figure 4: The EUROBALL experimental set up.

The γ-ray energies were measured with high-purity germanium (HPGe) semiconductor crystals. They were placed around the target according to figure 4 and they comprise 26 clover detectors, where each clover detector consist of four Ge crystals (see the insert to figure 4) and 15 cluster detectors, where each cluster detector consist of seven Ge crystals (see the insert to figure 4), which gives a total of 209 Ge crystals.

Important properties of a γ-ray detector array are the following:

- high efficiency in detecting incident γ-rays
- high resolution resulting in narrow energy peaks
- high ratio of full-energy to Compton scattered events, the so called peak-to-total ratio (P/T)
- high granularity to reduce the risk of detecting more than one γ-ray from the same event in the same detector

The HPGe detectors have these properties. The germanium crystal is provided with two electrodes in contact with the crystal material. When a γ-ray with energy E_γ enters the dector it interacts with the electrons in the crystal and the photon loses energy. If the photon is completely absorbed in the crystal it leaves all its energy to the electrons, which will give rise to a full-energy peak.

In many cases, however, the γ-photon does not deposit its whole energy to the electrons, but it Compton-scatters and disappears from the Ge crystal, leaving only a part of its energy. This partially deposited energy then gives rise to a continuous Compton background, which interfere with γ-ray lines of low energy (see figure 5).

To reduce the Compton background, each of the Ge detectors is surrounded by a shield of bismuth germanate scintillator crystals; BGO crystals. With these BGO crystals we measure the γ-ray energy from the disappearing photons. By rejecting events in which Compton-scattered γ-rays have left only a part of their energy in the Ge detectors these Compton Supression shields can increase the P/T ratio significantly. The effect of such a suppresion is shown figure 5 for the radioactive source of ^{60}Co.

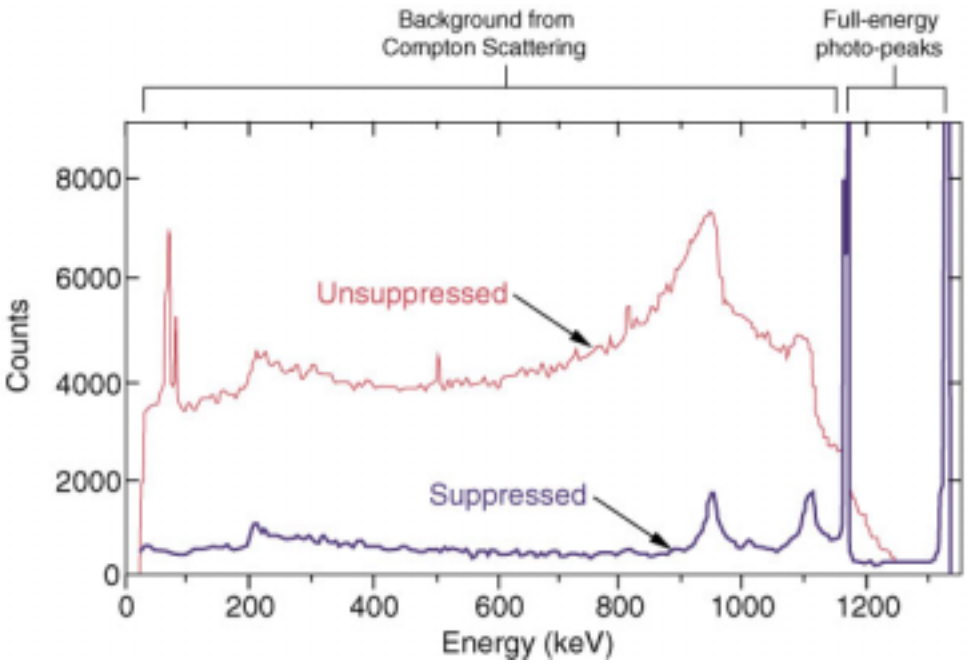

Figure 5: Illustration of the Compton Suppression Technique [5].

The singles count rate per Ge detector needs to be kept below about 10 kHz to reduce effects of pile-up of the relatively slow Ge energy signals. The singles γ-ray count rate in the present experiment can be estimated. The reaction rate, R, in the present experiment was estimated in the previous section to be about 10^5 s^{-1}. If one assumes an average multiplicity of 10 γ-rays per reaction the count rate per Ge detector, R_γ, will be

$$R_\gamma \le \frac{10R}{\#Ge\ crystals} = \frac{10 \cdot 10^5}{209} \approx 7\ kHz$$

If we would cover the whole solid angle of 4π with the Ge detectors, the inequality in the expression become an equality.

The efficiency for detecting γ-rays in the Ge detector decreases at high energies due to higher probability of energy loss by Compton scattering and at lower energies due to ab-

sorbation in the material between the target and the Ge crystals. A γ-ray efficiency calibration was therefore done. The well known radioactive source ^{152}Eu was used as a calibration source and from its known γ-ray intensities a calibration was fitted for the relative γ efficiency, ε_γ, according to:

$$\ln(100\varepsilon_\gamma) = \left\{ \left[k_1 + k_2 \ln\left(\frac{E}{100}\right) + k_3 \left(\ln\left(\frac{E}{100}\right) \right)^2 \right]^{k_7} + \left[k_4 + k_5 \ln\left(\frac{E}{1000}\right) + k_6 \left(\ln\left(\frac{E}{1000}\right) \right)^2 \right]^{k_7} \right\}^{\frac{1}{k_7}} \quad (1)$$

where E is the γ-ray energy and k_i are the fitted parameters.

The light charged particles were detected in an array of 40 $\Delta E/E$-telescope Si detectors placed in the centre of EUROBALL at a distance of about 15 cm from the target. Each telescope consists of two counters. The first counter is very thin (130 μm). The particles pass through it and loses only a small amount of their energy, ΔE. Since $\Delta E \propto Z^2$ (see equation 7.3 of ref [3]), where Z is the charge of the particle, the particles can be distinguished by the measurement of the energy loss in the thin counter. The second counter is thick enough to stop all protons and α-particles, which means that all their energy is deposited in the detector, E.

The Neutron Wall is an assembly of 50 liquid scintillator detectors covering a solid angle of about 1π in the forward direction with respect to the beam direction (see figure 4). The detection of neutrons is very important for selecting the very rare reaction channels leading to the most neutron deficient nuclei. This detector is also sensitive to γ-rays, and therefore it is important for such a detector to be able to discriminate between neutrons and γ-rays, which is done by a combined technique based on pulse shape discrimination and time-of-flight.

3 ANALYSIS AND RESULTS

A total of about 30 different residual nuclei in the mass region around A ~100 were populated in the present experiment (see figure 2). The main goal of the experiment was to search for excited states in the nucleus ^{103}Sn, but the many open channels in the reaction which was used makes this task very difficult. The data analysis becomes very complicated. The specific tasks of the present project work was

a) to determine the particle detection efficiency
b) to clean the spectra from contaminating lines
c) to determine the relative cross sections of the different reaction channels
d) to search for γ-ray lines in ^{103}Sn and finally
e) to determine the level scheme of ^{103}Sn.

3.1 Detection efficiency

Study the γ-ray spectrum in figure 6. It has been produced by requiring that three protons were detected in the Si-ball. One would therefore expect to see in this spectrum γ-ray transitions from the nucleus ^{109}Sb, because it is produced in the three proton (3p) reaction channel (see figure 2). This is also the case, and some of the strong lines in ^{109}Sb are marked in the spectrum in figure 6. However, in this spectrum we also observe lines from other populated nuclei. The two peaks at 1196 keV and 1206 keV are from ^{108}Sn, which is populated in the 4p reaction channel (see figure 2). Thus, four protons are evaporated in this reaction channel but one proton was missed in the detection, since we do not have

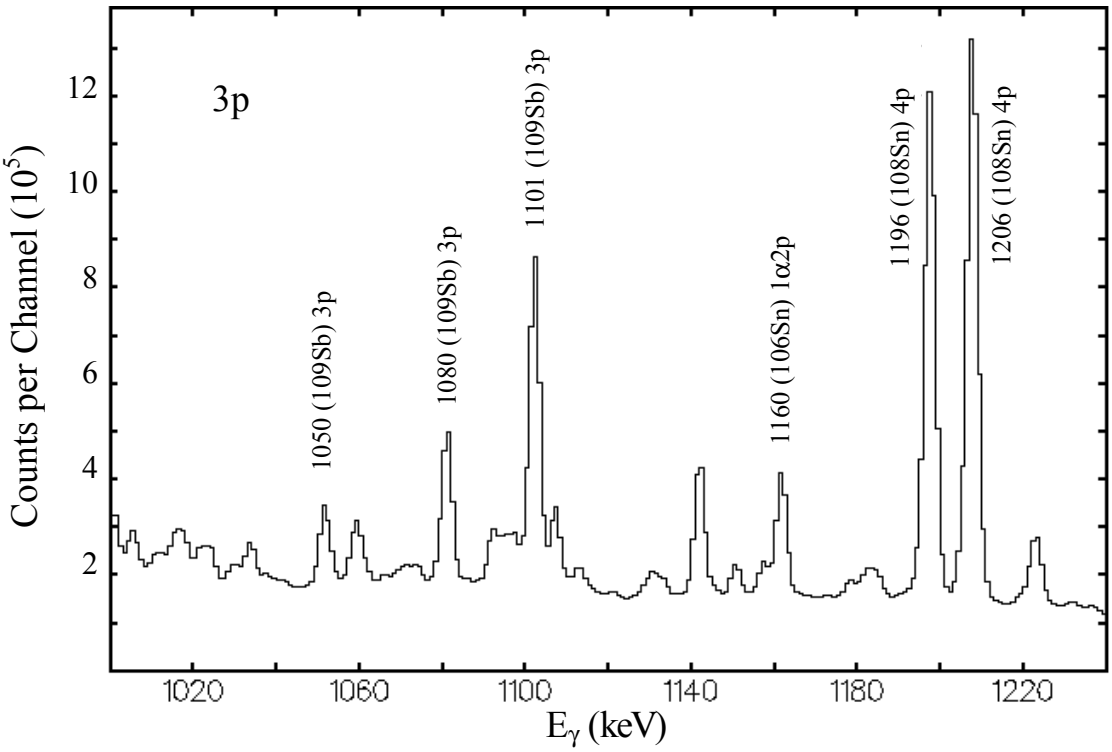

Figure 6: Part of the 3p gated spectrum with contaminations from the 4p- and 1α2p-channels.

100 % efficiency of detecting protons. Therefore γ-ray lines from the 4p channel (^{108}Sn) will be observed in the 3p gated spectrum. The 3p gated spectrum is contaminated by the ^{108}Sn γ-rays. The peak at 1160 keV in figure 6 originates from ^{106}Sn, which is populated in the 1α2p reaction channel. In this reaction, which emits one α-particle and two protons, there have been a misidentification between a proton and an α-particle. Again the occurrence of this reaction channel in the 3p gated γ-ray spectrum is a result of the particle detection not being perfect.

The difficulty due to the small detection efficiency is also illustrated in figure 7. It shows again a γ-ray line (1101 keV) which belongs to the nucleus ^{109}Sb corresponding to the 3p channel.

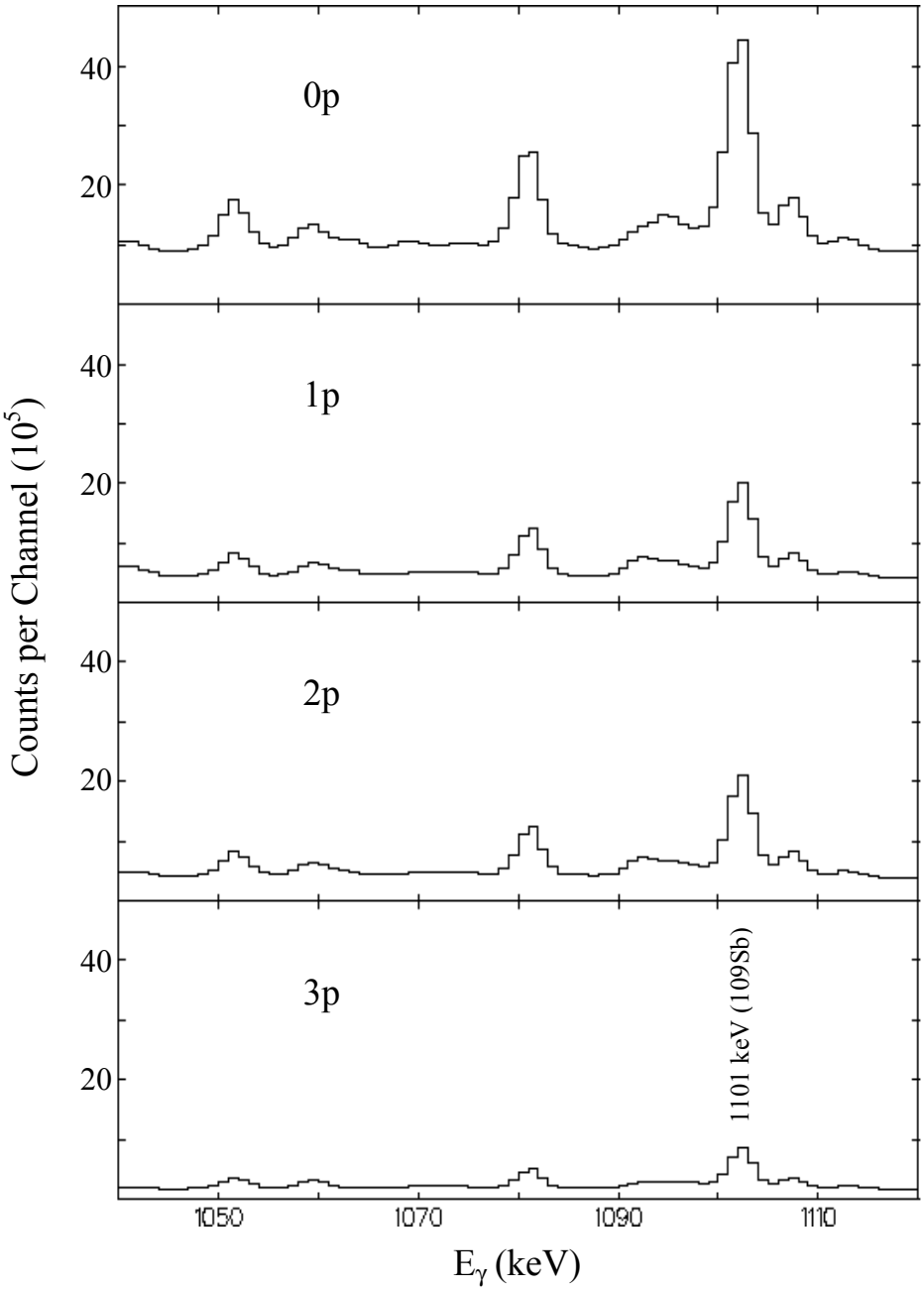

Figure 7: γ-ray spectra demanding that three, two, one and zero protons were detected in the Si ball. A peak from ^{109}Sb is seen at 1101 keV. Due to the limited particle detection efficiency the peak at 1101 keV is higher in the two, one and zero gated spectra than in the 3p gated spectrum, where it belongs.

Figure 7 shows that this line is observed also in the 2p gated spectrum as well as in the 1p and 0p gated spectrum. In fact, it is larger in the 0p, 1p and 2p gated spectra, where it does not belong, than in the 3p gated spectrum. This means that the intensity of a specific nucleus, in this example ^{109}Sb, is spread out over several different gated γ-ray spectra, which is a problem.

The intensities of the 1101 keV line as observed in the spectra gated with different number of protons can now be used to determine the efficiency for detecting protons in the Si-ball. If the particle detection efficiency had been 100 %, there would have been no intensity at all in the 1101 keV line in the 0p, 1p or 2p gated spectra. The whole intensity of the 1101 keV peak would have been in the 3p gated spectrum. On the other hand if the particle efficiency had been 0 %, we would have found all the intensity of the 1101 keV peak in the 0p gated spectrum.

The ratio of the intensity of a γ-ray line in ^{109}Sb as measured in the 3p- and in the 2p-gated spectra is proportional to the ratio of the probabilities to detect three protons and two protons respectively. As an example let's take the reaction channel in which three protons are being emitted. If the efficiency to detect one proton is ε, the complementary event, that no particle is detected, is $1-\varepsilon$ (see figure 8). Let us follow the leftmost branch of the tree in figure 8. It is marked 3p in the bottom and it represents the situation when all the three emitted protons are detected. There is only one branch in the binary tree in figure 8 that represent this case. The probability to detect all three protons is thus ε^3. The detection of two protons out of the three emitted can occur in different ways. The first case is when the two first protons are detected but the third proton is missed. This is the branch marked $2p_{(1;2)}$ and the probability for this branch is given by $\varepsilon^2(1-\varepsilon)$. The second case is when the first and the third proton is detected but the second proton is missed. This is the branch marked $2p_{(1;3)}$ and the probability for this branch is given by $\varepsilon(1-\varepsilon)\varepsilon$. The third case finally, is when the second and the third proton is detected, $2p_{(2;3)}$. The probability for this branch is given by $(1-\varepsilon)\varepsilon^2$.

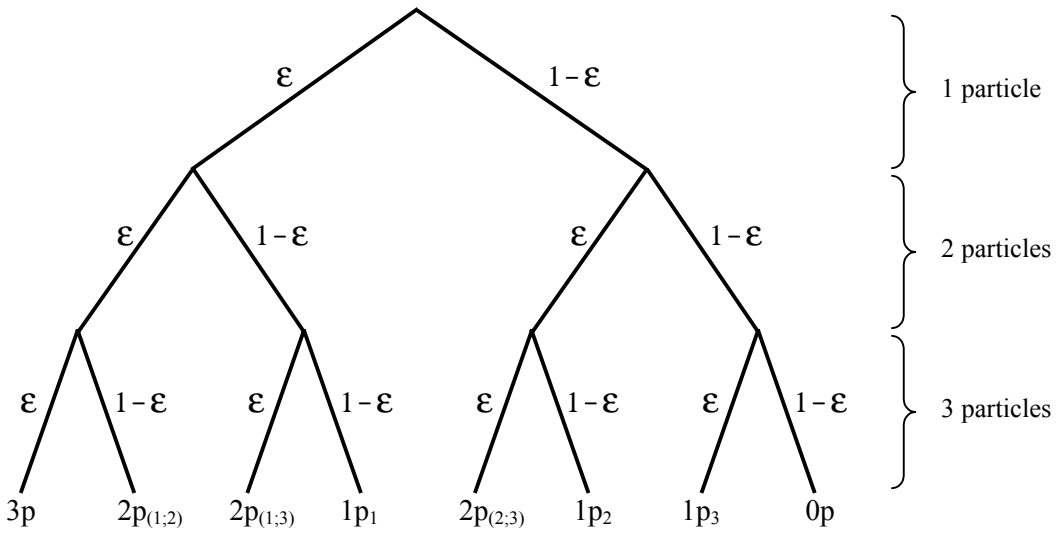

Figure 8: The binary tree showing the distribution of the propabilities for detecting zero, one, two or three particles in the emission of three particles.

Thus the total probability to detect two protons when three are emitted is the sum of these three branches, i.e. $3\varepsilon^2(1-\varepsilon)$. Similarly the probability to detect only one proton out of three emitted is given by $3\varepsilon(1-\varepsilon)^2$ (see the branches marked with $1p_1$, $1p_2$ and $1p_3$). Thus the ratio R of the intensities of one γ-ray line in ^{109}Sb as observed in the 3p and the 2p gated spectra is given by

$$R = \frac{I(^{109}Sb)_{3p}}{I(^{109}Sb)_{2p}} = \frac{\varepsilon^3}{3\varepsilon^2(1-\varepsilon)} = \frac{\varepsilon}{3(1-\varepsilon)}$$

where $I(^{109}Sb)_{3p}$ is the intensity of ^{109}Sb in the 3p gated spectrum and $I(^{109}Sb)_{2p}$ is the intensity of ^{109}Sb in the 2p gated spectrum. This gives the efficiency for detection of protons in the present experiment.

Assume that the detection efficiency is 50 %. The propability P to detect three particles with an emission of three particles is then $P(3) = 0.5^3 = 1/8$. The propability to detect two particles out of the three is $3 \cdot 0.5^2(1\text{-}0.5) = 3/8$. From figure 8 we also see that the probability to detect one or zero particles out of the three emitted is 3/8 and 1/8 respectively. These numbers are the well-known binomial coefficients. If we again look at figure 7, we see that the intensitiy of the 1101 keV line, the 3p-, 2p- and 1p gated spectra is approximately 1:3:3, i.e. they are the same as the probabilities above; the binomial coefficients. The value in the 0p gated spectrum is not reliable because the zero particle requirement makes this spectrum too much contaminated. From this simple exercise we can already conclude that the efficiency for proton detection is close to 50 %.

A more general expresion for the ratio of intensities is

$$R = \frac{I\left({}^{A}_{Z}X\right)_{np}}{I\left({}^{A}_{Z}X\right)_{kp}} = \frac{1}{\binom{n}{k}} \cdot \frac{\varepsilon^{n-k}}{(1-\varepsilon)^{n-k}} \qquad (2)$$

where n is the number of emitted particles, k is the number of particles in the gated spectrum that we compare to, k = 0, 1,…, n - 1, and (n over k) are the binomial coefficients, given by $n!/[k!(n\text{-}k)!]$.

We can now determine the proton efficiency in the present experiment more accurately. In this determination the γ-ray intensity of the 905 keV line in the nucleus ^{108}Sn was studied (see table 1). ^{108}Sn is populated in the 4 proton channel and γ-rays from ^{108}Sn was thus observed in the 4 proton gated spectrum as well as in the 3p, 2p, 1p and 0p gated spectra. The ratio *R* between some combinations of those spectra are determined and shown in table 1. For each of these values *R* the proton efficiency ε_p is determined. As can be seen they all lie around 50 %. The same exercise was applied also to the γ-ray intensity of the 312 keV line in the nucleus ^{108}Sb (see table 1). In seven of these twelve determinations the equation (2) was used.

The proton efficiency value 0.36 (see table 1) we consider less reliable, since as mentioned above the 0p gated spectrum is very contaminated. An average value, excluding the 0.36 value, the proton efficiency, ε_p, is estimated to be 51 %.

^{108}Sn(E_γ = 905 keV)			^{108}Sb(E_γ = 312 keV)		
*n*p/*k*p	*R*	ε_p	*n*p/*k*p	*R*	ε_p
4p/3p	0.27	0.52			
4p/2p	0.18	0.51			
4p/1p	0.21	0.49			
4p/0p	0.10	0.36			
3p/2p	0.66	0.47	3p1n/2p1n	0.42	0.56
3p/1p	0.78	0.47	3p1n/1p1n	0.37	0.51
3p/0p	0.37	0.53	3p1n/0p1n	0.32	0.41
2p/1p	1.18	0.49	2p1n/1p1n	0.90	0.64

Table 1: Ratios and efficiency values for calculation of the proton efficiency.

The α-efficiency, ε_α, was determined similarly. From the ratios of the 200 keV and 1194 keV lines, which are strong lines in ^{105}Sn, as measured in the 1α2p1n- and 2p1n-spectra, ε_α was determined to about 33 %. The neutron efficiency, ε_n, was determined to 87 % from the intensity ratio of five different γ-ray energies of 3p1n/3p spectra.

3.2 Cleaning the spectra

The next thing to do in the analysis was to clean the spectra from their contaminations. Figure 9a, which is the same as figure 6, shows the uncleaned 3p gated spectrum again. As discussed in section 3.1 this spectrum contains γ-ray lines also from the 3p1n, 1α3p, and 4p1n reaction channels. The cleaning was done by subtracting, with proper normalization constants, the 3p1n, 1α2p, 1α3p, 4p and 4p1n gated spectra. The normalisation constants

were determined by measuring the area in the peaks, i.e. the intensities, of a strong γ-ray transition of the contaminating channel. In this case four of the five spectra were cleaned in a similar way before the subtraction. Figure 9b shows what is left after the subtraction, i.e. a nicely cleaned spectrum, which mainly contains γ-ray lines from ^{109}Sb. This cleaning procedure was done on all the 30 channels that were open in the reaction.

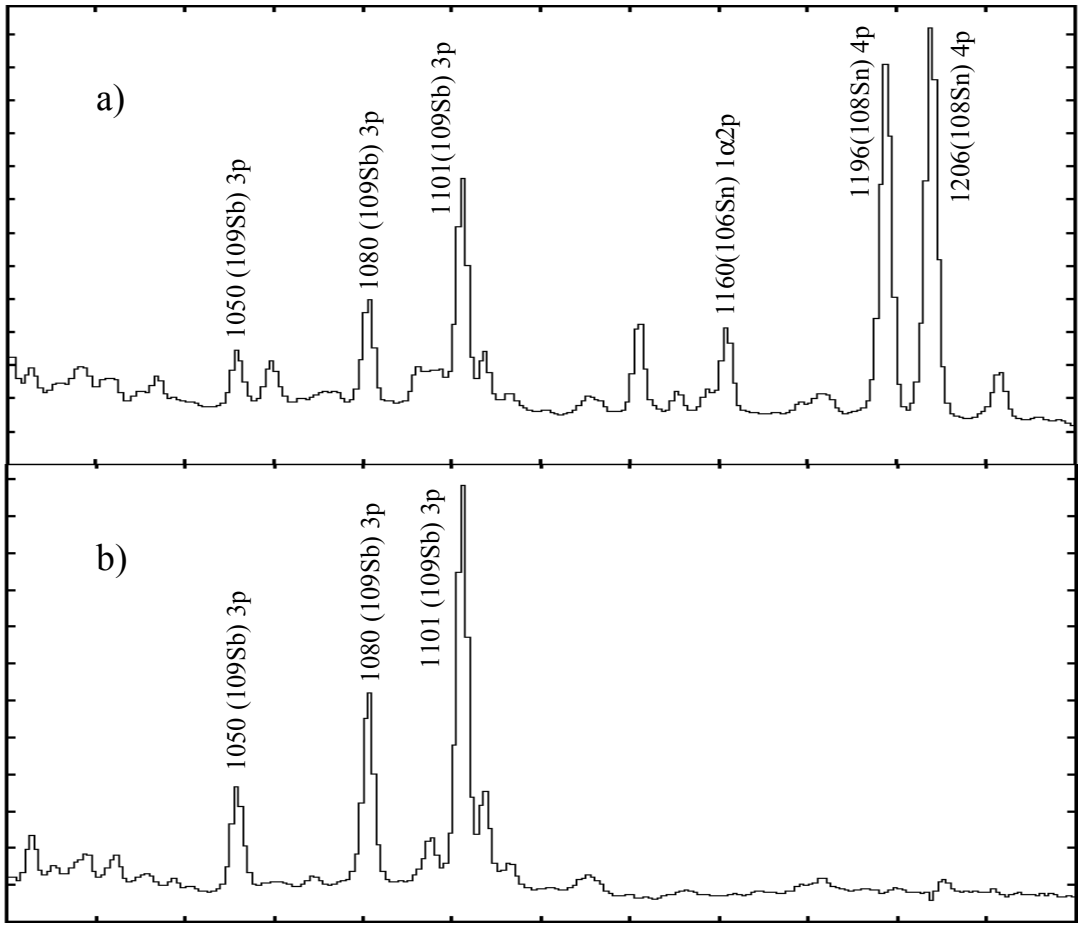

Figure 9: A comparison between the uncleaned and the cleaned 3p gated spectrum.

To find γ-ray transitions belonging to the weakly populated nucleus ^{103}Sn it was necessary to clean the 2α1n spectrum from its contaminating channels as much as possible. For such a weak channel it is important to perform this work very carefully. The 2α1n spectrum was subtracted by the 2α1p1n, 1α2p1n, 2α2p1n and 1α2p gated spectra with proper normalisation constants. The 1α2p channel is a relative strong channel, see figure 2, so dispite the requirement of one neutron less, it appeared in the 2α1n spectrum, as random coincidences. Also the 1α2p1n channel, a strong channel compared to the 2α1n channel, contaminated ^{103}Sn with random coincidences. Each of these four spectra was at this stage already cleaned and they were therefore very useful to clean the ^{103}Sn spectrum.

Figure 10 shows the cleaned ^{103}Sn spectrum in the region 0 keV ≤ E_γ ≤ 1500 keV. This will be discussed in more detail in section 3.4.

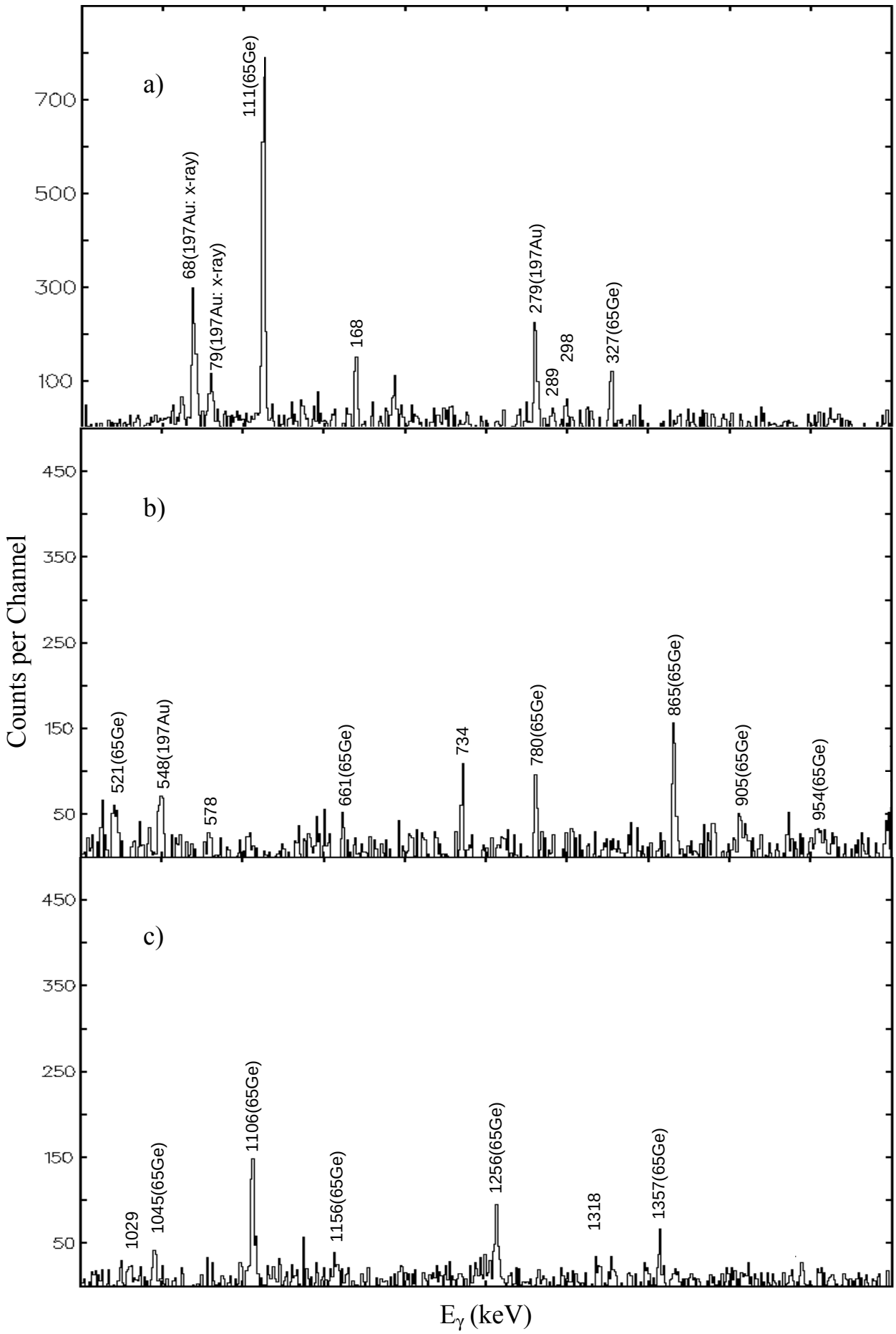

Figure 10: The cleaned ^{103}Sn spectrum in three different regions of the γ-ray energy.
Top: ($0 \le E\gamma < 500$) keV. Middle: ($500 \le E\gamma < 1000$) keV. Bottom: ($1000 \le E\gamma < 1500$) keV.

3.3 Cross Section determination

The propability of a nuclear process to occur is often expressed in terms of a cross section σ which has the dimension of an area. For two nuclei passing each other (see figure 11) the geometrical cross section is defined as

$$\sigma_{geometric} \equiv \pi(R_1 + R_2)^2$$

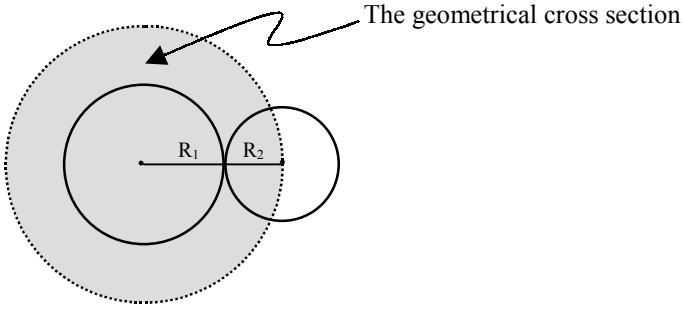

Figure 11: A schematic picture of the geometrical cross section, $\sigma_{geometric}$.

With the empirical formula for the radius of a nucleus with mass number *A*

$$R = r_0 A^{1/3} \qquad r_0 \approx 1.2 \cdot 10^{-15} m$$

the geometrical cross section is given by

$$\sigma_{geometric} = \pi r_0 \left(A_1^{1/3} + A_2^{1/3}\right)^2$$

In the present experiment the geometrical cross section for ^{58}Ni and ^{54}Fe is about $2.6 \cdot 10^{-24}$ cm^2 = 2.6 b. This is a rough estimate of the reaction cross section, and only an upper limit. One must also take into account that there are charged particles involved that have to overcome Coloumb barriers, and there may be structure effects. In fact, the cross section depends on many parameters. A computer programme called CASCADE [6] treats the reaction in a statistical way and using it the total reaction cross section was calculated to about 0.5 b.

The *relative* cross section of the different open reaction channels can be determined from the experimental relative yield *y* of the populated nuclei, which is proportional to the γ-ray intensity. For the even-even nuclei the intensity was determined from the γ-ray transition from the first excited state to the ground state and for the odd nuclei the intensities of all transitions going to the ground state were summed. The yield y_i of a certain reaction channel is thus given by

$$y_i = \frac{I^{corr}}{\varepsilon_p^i \cdot \varepsilon_\alpha^j \cdot \varepsilon_n^k}$$

where ε_p, ε_α and ε_n are the efficiencies for detection of the light particles determined in section 3.1 and I^{corr} is the corrected γ-ray intensity according to

$$I^{corr} = \frac{I}{\varepsilon_\gamma}$$

where I is the area of the γ-ray peak and ε_γ is the relative γ-ray efficiency factor given by equation (1). The total yield Y_{tot} is given by the sum of all the partial yields according to

$$Y_{tot} = \sum_i y_i$$

and the relative cross section σ_{relative} is thus given by

$$\sigma_{relative} = \frac{y_i}{Y_{tot}}$$

For example; the intensity of the γ-ray transition to the ground state at 658 keV in the nucleus ^{104}Cd in the 1α4p channel was measured to be 4778 counts. From equation (1) the γ-ray efficiency was calculated to 2.03 given I^{corr} = 2346. With the efficiency values, ε_α = 0.33 and ε_p = 0.51 the yield is given by

$$y_{1\alpha 4p} = \frac{2346}{0.33 \cdot 0.51^4} = 113\ 745$$

This gives a relative cross section of 0.2 % for the 1α4p channel. The low cross section is expected, since this particular channel emits five particles, one α-particle and four protons, which is not a very probable process at a beam energy of only 240 MeV. This emission would have a larger propability if the compound nucleus could be produced at higher energy.

In this nuclear reaction the most probable emissions are containing three to four particles. Figure 2 shows that strong channels are the 3p1n, 3p, and 4p channels, populating ^{108}Sb, ^{109}Sb and ^{108}Sn, respectively. For some of the nuclei there are more than one evaporation channel that can populate it. For instance; ^{106}Sn will also, besides the 1α2p gated channel, be populated by emission of four protons and two neutrons, but the cross section for that reaction channel is extremly small. 16 of the identified populated nuclei have cross sections of less than 5 mb. Weak channels are the 3α, 2α1n and 2α2p1n channels but also the 1p channel populating ^{111}I (see figure 2).

No γ-ray transitions were known in ^{103}Sn before the present investigation. One possible candidate for a transition is the 168 keV transition (see section 3.4). From a measurement of the intensity of this γ-ray line at 168 keV in the 2α1n spectrum a relative cross section for ^{103}Sn was determined to 0.004 %.

In figure 12 the logarithm of the relative cross section is plotted as a function of the number of protons. For every graph the number of neutrons and α-particles are constant, i.e. every graph is a column in the nuclidic chart of figure 2. The notation 0α0n for example, means that no α-particles and no neutrons are emitted besides the protons and 0α1n means that one neutron is emitted besides the protons.

For each graph the diagram shows some symmetry in the way the evaporated nuclei are populated with respect to the protons. Many evaporated protons, as well as few, like the 1p channel mentioned above, give a small cross section. For every graph there is a maximum somewhere in the middle.

The 0α0n-graph has its maximum at about 3.5 protons and the 0α1n-graph has its maximum at about 3 protons. For each graph the maximum cross section is obtained for approximately 3 or 4 emitted particles. The difference between the largest and the smallest

cross section is about four orders of magnitude. ^{103}Sn, the 2α1n0p channel, is seen in the y-axis.

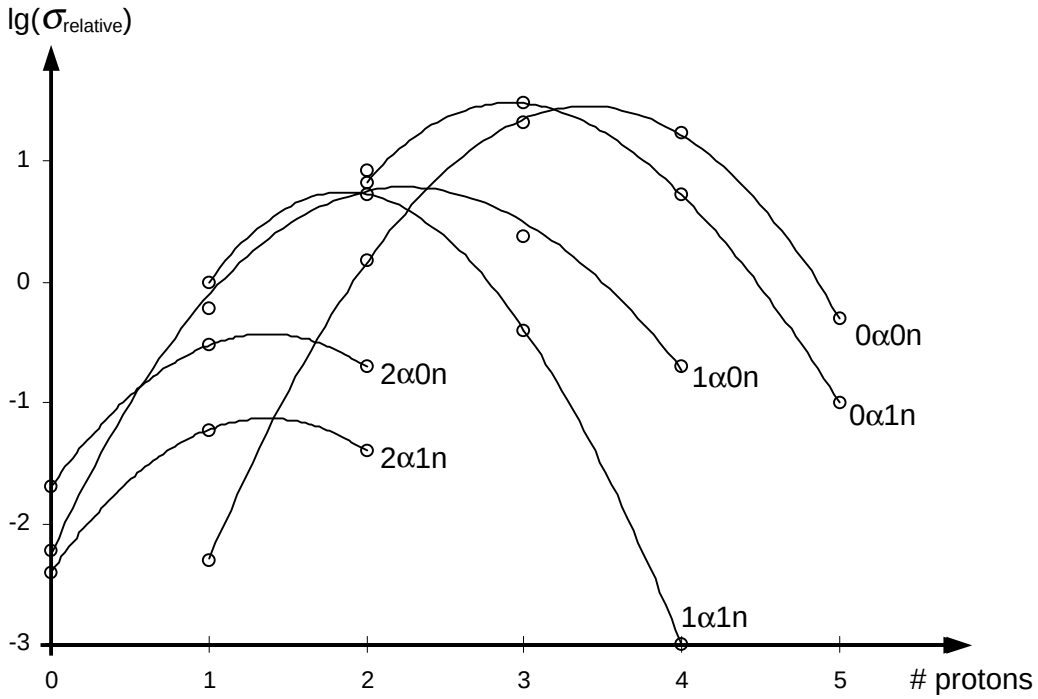

Figure 12: The logaritmic cross section as a function of the number of protons for different values on emitted α-particles and neutrons.

3.4 Identification of γ-ray lines in ^{103}Sn

Figure 10 shows the cleaned 2α1n gated spectrum. The cleaning was done by subtracting, with proper normalisation constants, the 2α1p1n, 1α2p1n, 2α2p1n and 1α2p gated spectra. The two energy lines at 68 keV and 79 keV in figure 10a are identified as x-rays from the ^{197}Au. After the ^{58}Ni beam has passed through the ^{54}Fe plate it comes into the Au backing with a current of about 10^{10} s^{-1}. When electrons in the gold atoms are hit by the Ni ions - the propability for that is large because the atomic cross sections are large compared to the nuclear cross sections - they excitate the electrons to a higher level and during their deexcitation they send out x-rays. These Au x-rays are seen in the spectra as random coincidences.

A small number of the beam nuclei are going straight forward the Au nuclei into a head on collision. Since Z(Au) = 79, a ^{58}Ni nucleus with an energy of 240 MeV will never reach the Au nucleus but due to the Coloumb barrier turns off and passes by the Au-nucleus. The electromagnetic field that arises at the transit causes a Coloumb excitation in the Au nucleus resulting in excitated states of Au and this is the reason for the γ-ray lines at 279 keV and 548 keV (see figure 10a and figure 10b).

Since it is not possible to construct a perfect vacuum the ^{58}Ni beam also will react with the oxygen being built up on the target according to $^{58}Ni + {}^{16}O \rightarrow {}^{74}Kr^*$. One reaction

channel for the compound nucleus ^{74}Kr to decay is to emit two α-particles and one neutron, populating ^{65}Ge. This reaction is the origin to the γ-ray lines at 111 keV and 327 keV in figure 10a, the γ-ray lines at 521, 661, 780, 865, 905, 954 keV in figure 10b and the γ-ray lines at 1045, 1106, 1156, 1256, 1357 keV in figure 10c.

The remaining γ-ray lines in Figure 10 at 168, 289, 298, 578, 1029 and 1318 keV have not been identified from other level schemes. These six lines are candidates for γ-ray lines in ^{103}Sn.

3.5 Experimental level scheme of ^{103}Sn

To confirm that these six γ-ray lines really belong to ^{103}Sn it is necessary to make a γγ coincidence matrix. This means that we have to put a gate on one of the γ-ray lines, for instance the 168 keV line, and see if the other γ-ray candidates are in coincidence with this line.

Since a master thesis project is strongly limited in time, there was no time to perform this last step in the data analysis. However, this γγ gating analysis has been done parallel by other members of the Nucleur Structure Group. It has been established that that these six γ-ray lines are in coincidence with each other and it has been concluded that the γ-ray lines proposed in the present project work actually belong to ^{103}Sn.

From the present analysis and from the coincidence-relationships we have determined the energy level scheme for ^{103}Sn according to figure 13. The result is going to be published [7].

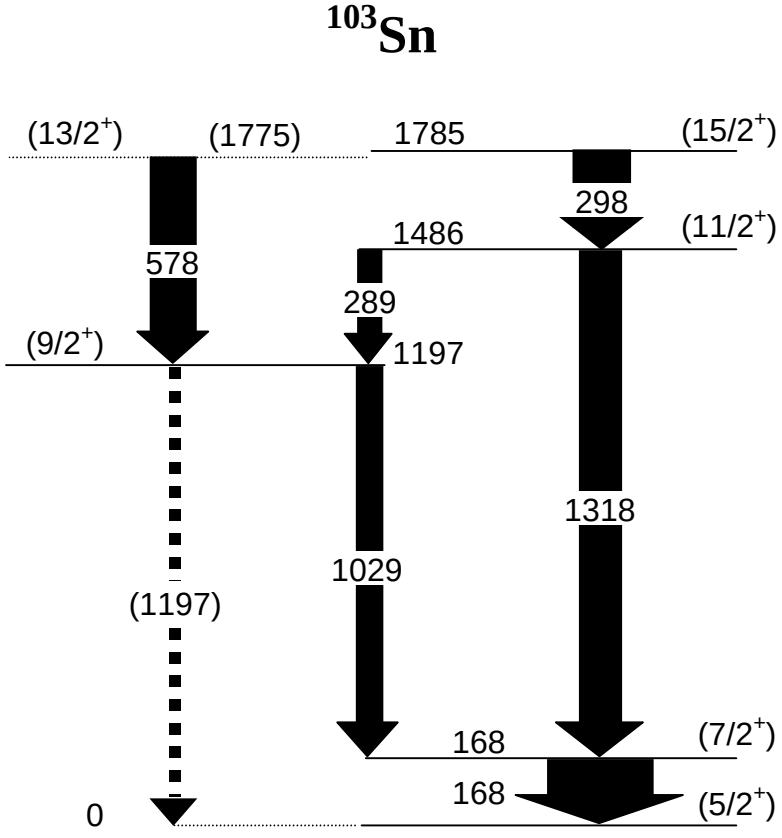

Figure 13: The proposed level scheme of ^{103}Sn. The widths of the arrows correspond to the relative intensities of the transitions.

From the cleaned 2α1n spectrum the intensities are experimentally determined and the widths of the arrows in figure 13 correspond to the relative intensities of the transitions. The most intensive γ-ray line of the six candidates is the 168 keV line (see figure 10). It is therefore placed in the bottom of the level scheme.

The spin and parity of the ground state is not known from previous measurments. However, we suggest it has spin and parity $5/2^+$ based on systematics from earlier experiments in ^{105}Sn, ^{107}Sn and ^{109}Sn. By using angular distributions of γ-rays the spin and parity of the other states are experimentally determined (see figure 13).

4 SHELL MODEL CALCULATIONS

^{103}Sn consists of 50 protons and 53 neutrons. 50 is a magic number and from the shell model the magic numbers represent the closing of a major shell [3] in analogy to the electron shells in the atomic theory. When a nucleus has either a major proton or neutron shell filled, it is more stable than its neighbours, since the energy gap to the next shell is large. A shell is defined as several energy levels lying close together, clearly separated from other shells.

The nuclear shell model assumes that the nuclear properties are determined primarily by the valence nucleons, i.e. by the particles outside the closed shells. This means that in ^{103}Sn in a first approximation the filled proton shells do not contribute to the structure. The properties of the ground state and the first excited states are determined only by the three valens neutrons (see figure 14).

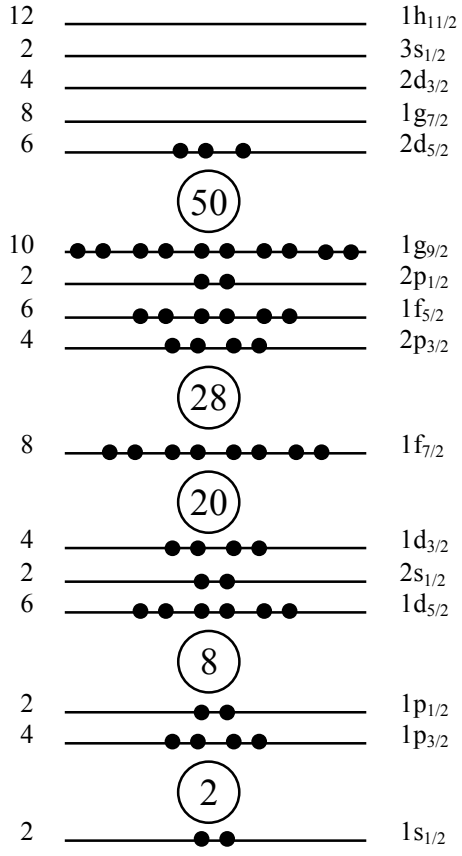

Figure 14: The neutron configuration of the ground state in ^{103}Sn.
The black dots illustrates the neutrons, 53 altogether.

Quantum mechanically every nucleon can be labelled with the corresponding quantum numbers n, l, s, j and m_j. The notations to the right of each level in figure 14 are the quantum numbers n, l and j, where n is the radial quantum number. As in the atomic theory the

notation for the orbital angular momentum l are denoted by the symbols l = s, p, d, f, g,… corresponding to the values l = 0, 1, 2, 3, 4,… and so on. Nucleons, like electrons, have intrinsic spin quantum numbers of 1/2. A nucleon with angular momentum l and spin *s* has a total angular momentum $\boldsymbol{j} = \boldsymbol{l} + \boldsymbol{s}$. This l *s*-coupling leads to a splitting of each *n*l state into two states with $j = l + 1/2$ and $j = l - 1/2$. The numbers to the left in figure 14, given by $2j+1$, show the capacity of each level, i.e. the total number of particles in one orbital according to the Pauli principle. The Pauli principle is explained below. The numbers 2, 8, 20, 28 and 50 are some of the magic numbers representing filled major shells [3].

The total angular momentum of a nucleus containing *A* nucleons would be the vector sum of the angular momenta of all the nucleons. The total angular momentum is represented by the symbol *I*. For ^{103}Sn the nuclear total angular momentum will be

$$\vec{I} = \sum_{i=1}^{103} \vec{j}_i$$

In the simplest form of the nuclear shell model only the effects due to the last unpaired single particle is taken into consideration. All protons and the first 52 neutrons in ^{103}Sn are coupled anti-parallel two by two since it costs the least of energy, given the vector sum

$$\vec{I} = \sum_{i=1}^{102} \vec{j}_i = 0$$

In a more realistic approach, where we include all three valence neutrons outside the filled 50 shell (see figure 14), the nuclear spin will be $\mathbf{I} = \mathbf{j_1} + \mathbf{j_2} + \mathbf{j_3}$ for ^{103}Sn. This will give a much richer spectrum of excited states. However, let us for simplicity confine the study to the two lowest orbitals outside the filled 50 shell, i.e. to the $2d_{5/2}$ and $1g_{7/2}$ orbits. There are only four possible ways to place three neutrons in these two orbits, i.e. four possible configurations. They are shown in figure 15.

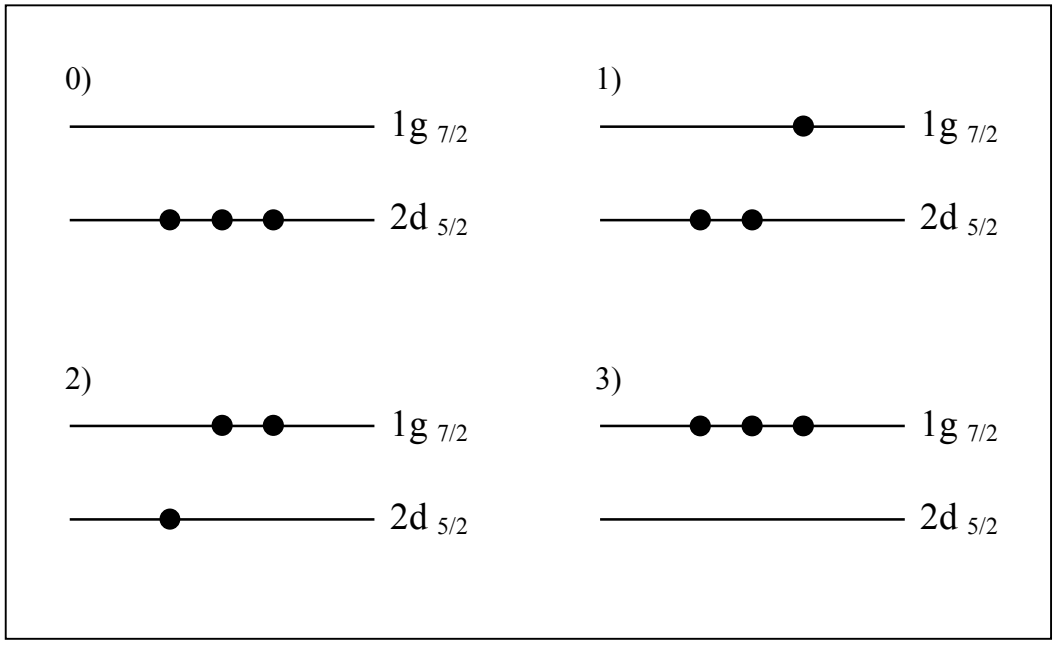

Figure 15: The three valence neutrons in ^{103}Sn in four different modes. $2d_{5/2}$ and $1g_{7/2}$ are the two lowest levels in the sixth major shell.

Which spins are possible from each of these four configurations with three neutrons involved? Let us start with figure 15:0. Each of these neutrons have, in the shell model, angular momentum $j = 5/2$, which can have the projections on the z axis $m = \pm 1/2,\ \pm 3/2,\ \pm 5/2$. The maximum value of the total projection, $M = m_1 + m_2 + m_3$, for the three neutrons is +15/2. However, the nucleons are fermions, which means that they have half-integer spins and they must obey the Pauli exclusion principle. The Pauli principle says that no two particles can have the same set of quantum numbers, i.e. two identical nucleons cannot be in the same quantum state. A consequence will be that each of the three neutrons in $2d_{5/2}$, since they have the same value of $j = 5/2$, must have a different value of the quantum number m. The maximum value of M will therefore be +5/2 +3/2 +1/2 = 9/2. Since $-M < I < M$, we expect to find no state in configuration 15:0, the configuration $(d_{5/2})^3$, with I

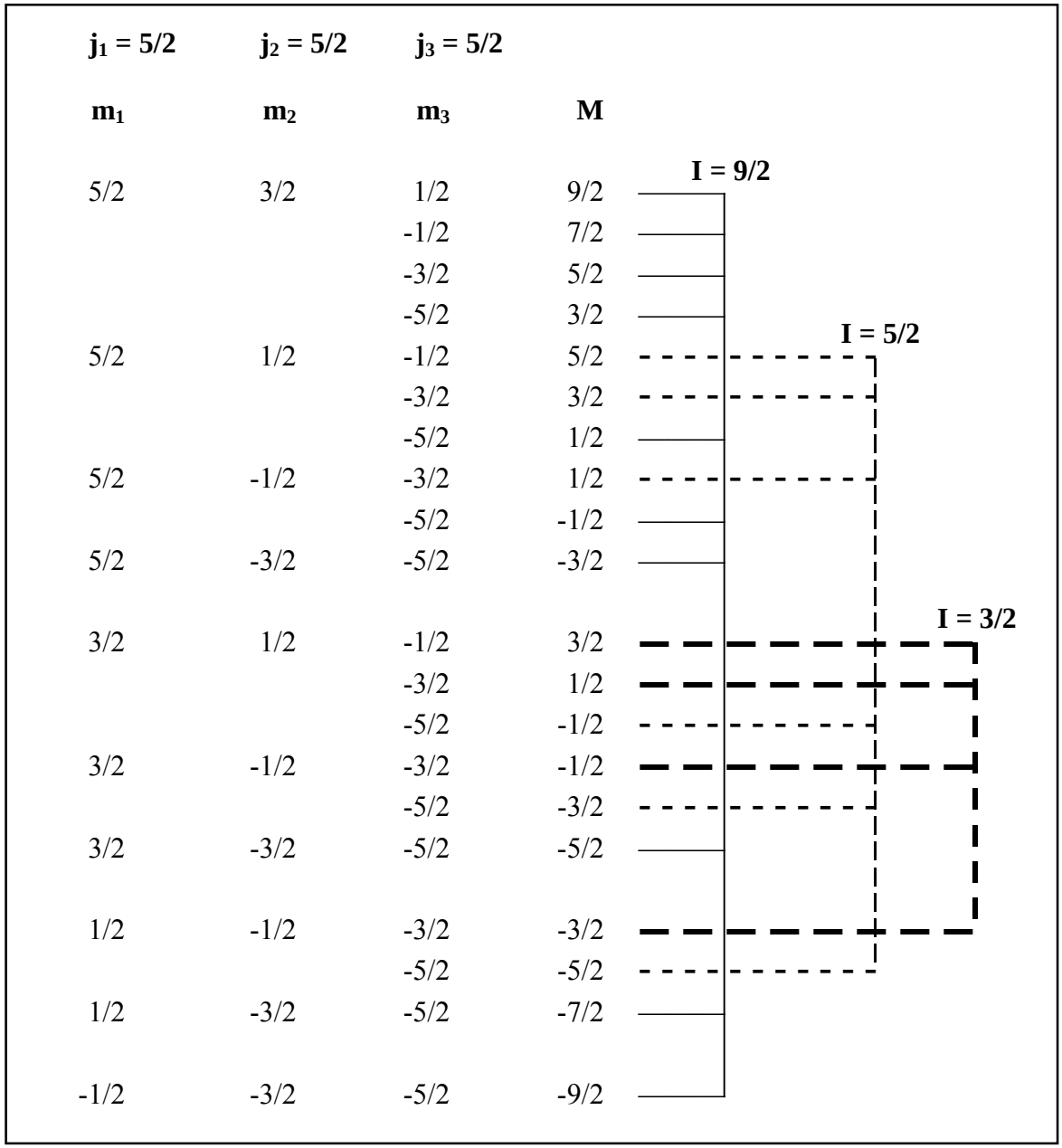

Figure 16: The three neutrons in the $2d_{5/2}$ orbital with j = 5/2 each. According to the Pauli exclusion principle the possible total angular momentum will be I = 9/2, 5/2 and 3/2.

greater than 9/2. This maximum resultant $I = 9/2$, can have all possible M from +9/2 to -9/2 (see figure 16).

The next highest possible M is +7/2, which can be obtained from +5/2 +3/2 -1/2 (+3/2 +3/2 +1/2 is not allowed, nor is +5/2 +5/2 -3/2). This single $M = 7/2$ state must belong to the M states which we have already assigned to the $I = 9/2$ configuration. This means that we have no possibility to have a state with angular momentum $I = 7/2$. If we continue, we find two possibilities to obtain $M = +5/2$ (+5/2 +3/2 -3/2 and +5/2 +1/2 -1/2). One of these two possible $M = +5/2$ states is for the state with angular momentum $I = 9/2$ and another we can assign to a state with angular momentum $I = 5/2$. Finally, for configuration $(d_{5/2})^3$ there are three possible states with $I = 9/2$, 5/2 and 3/2 (see figure 16).

Figure 15:1 shows a configuration where one neutron is promoted to the $g_{7/2}$ level. The angular momentum values for the three neutrons in this configuration are: $j_1 = 5/2$, $j_2 = 5/2$ and $j_3 = 7/2$. If we first determine the spin for the two neutrons in the $d_{5/2}$ orbit, the spin is given by the rule: $|5/2 - 5/2| \le I \le 5/2 + 5/2$ N $I = 0, 1, 2, 3, 4, 5$. However, due to the Pauli principle not all of these values are allowed. The same calculations and using similar arguments as above the allowed states for the two neutron configuration $(d_{5/2})^2$ are $I = 0, 2, 4$. The parity positive. To these three spin values we couple the third neutron in the $g_{7/2}$ state according to

$|0 - 7/2| \le I \le 0 + 7/2$ N $I = 7/2$.
$|2 - 7/2| \le I \le 2 + 7/2$ N $I = 3/2, 5/2, 7/2, 9/2, 11/2,$
$|4 - 7/2| \le I \le 4 + 7/2$ N $I = 1/2, 3/2, 5/2, 7/2, 9/2, 11/2, 13/2, 15/2.$

Figure 15:2 shows the excited state where two neutrons are excited to the $g_{7/2}$ level. With the same arguments as above we get for the two neutrons in the $g_{7/2}$ orbit the allowed states of $I = 0, 2, 4, 6$. Coupling the $d_{5/2}$ neutron to these values gives nine different values in nineteen combinations. Table 2 shows all the allowed angular momentum values for the four configurations.

In the shell model the parity of the states are given by $\pi = (-1)^l$ and the resultant parity is the product according to

$$\pi = \prod_{i=1}^{A} \pi_i = \Pi(-1)^l$$

The ground state in ^{103}Sn has the l -value 2. The resultant parity $\pi = (-1)^2(-1)^2(-1)^2$ = positive parity. Since both *d* and *g* are even (l = 2 and l = 4) the parity will be positive in all four configurations.

configuration	$1/2^+$	$3/2^+$	$5/2^+$	$7/2^+$	$9/2^+$	$11/2^+$	$13/2^+$	$15/2^+$	$17/2^+$
$(d_{5/2})^3$		X	X		X				
$(d_{5/2})^2_{0^+} + g_{7/2}$				X					
$(d_{5/2})^2_{2^+} + g_{7/2}$		X	X	X	X	X			
$(d_{5/2})^2_{4^+} + g_{7/2}$	X	X	X	X	X	X	X	X	
$d_{5/2} + (g_{7/2})^2_{0^+}$			X						
$d_{5/2} + (g_{7/2})^2_{2^+}$	X	X	X	X	X				
$d_{5/2} + (g_{7/2})^2_{4^+}$		X	X	X	X	X	X		
$d_{5/2} + (g_{7/2})^2_{6^+}$			X	X	X	X	X	X	X
$(g_{7/2})^3$		X	X	X	X	X		X	

Table 2: By the use of the shell model fourtytwo states in the two lowest orbitals in ^{103}Sn are calculated.

5 DISCUSSION

By taking only the two lowest orbital into consideration we have, theoretically, by using the shell model, calculated forty-two states in ^{103}Sn with angular momentum ranging from $1/2^+$ to $17/2^+$ (see table 2). If we had taken into account all five orbitals in the sixth major shell (see figure 14) then we would have got many more theoretical states. Experimentally we have observed only six states in ^{103}Sn with angular momentum from $(5/2^+)$ to $(15/2^+)$.

The ground state of ^{103}Sn has been suggested to have spin and parity $5/2^+$. From table 2 we see that $5/2^+$ can theoretically be obtained in eight different ways from the four configurations of the two lowest orbitals only. Since it costs least energy to have all three neutons in the $d_{5/2}$-state our suggestion is that the ground state configuration is $(d_{5/2})^3$. However, this configuration, as seen in table 2, gives rise to three different angular momenta states. Which is the lowest? The pairing force that couple two of the three valence neutrons is strong and it costs much energy to break the pair. The most energetically favorable is when the two neutrons do not break the pair but couple the angular momentum to zero; one spin up and one spin down. Since each of the three neutrons in this configuration have angular momentum $j = 5/2$ the resultant will be $5/2^+$, which is our suggestion.

The first excited state has been suggested to be the 168 keV state with spin and parity $7/2^+$ (see figure 13). Theoretically we have seven different $7/2^+$ states (see table 2).

From experiments we know that even-even nuclei have angular momentum and parity 0^+ in the groundstate. The lowest energy is when two particles are coupled anti-parallel two by two; one spin up and one spin down. This means that a 2^+, 4^+ or 6^+ state costs more energy than a 0^+ state.

To break a pair costs more energy than to arise one particle to the $g_{7/2}$ state due to the very strong pair force. When all three neutrons are promoted to the $g_{7/2}$ state no pair is broken. The neutron pair in the $7/2^+$ state can be coupled to 0^+ which means that this is a low energy state. From this discussion we see that there are two configurations left for the $7/2^+$ state, namely $(d_{5/2})^2_{0^+} + g_{7/2}$ and $(g_{7/2})^3$. Since we do not break any pair in $(d_{5/2})^2_{0^+} + g_{7/2}$ configuration and arise only one neutron to the $g_{7/2}$ state we suggest this configuration to the $7/2^+$ state.

From this study we cannot say anything more about the other states. The situation is too complex in the $9/2^+$, $11/2^+$, $13/2^+$ and the $15/2^+$ states. We have pointed out but we cannot, without more elaborate shell model calculations, determine the most probable configuration. It can be done, but it is outside the scope of this work.

ACKNOWLEDGEMENTS

I would like to thank my supervisor Professor Claes Fahlander for the very professional and friendly guidance, advice and help during the progress of this work. I appreciate the way Claes has explained difficult subjects in an easy way. Many thanks also to Dr. Dirk Rudolph and Dr. Margareta Hellström for the time they have spent giving me lessons in nuclear physics.

REFERENCES

[1] D.Seweryniak, *Experimental Studies of Nuclei Near Doubly Magic ^{100}Sn,* Acta Universitatis Upsaliensis, 1994

[2] M. Lipoglavsek, *Rigidity of the Double-Magic ^{100}Sn Core,* Ph. D. thesis, Lund University, 1998

[3] K. K. Krane, *Introductory Nuclear Physics,* Wiley & Sons, 1988

[4] G. Friedlander, J. W. Kennedy, E. S. Macias, J. M. Miller, *Nuclear and Radiochemistry,* John Wiley & Sons, 1981

[5] Gammasphere Users Executive Committee, *Gammasphere The Beginning…1993 - 1997,*

[6] F. Pühlhofer, *Nucl. Phys.* **A280** (1977) 267

[7] C. Fahlander et. al, to be published.